Changes in Concrete Subjected to Neutron Irradiation

Zbyněk Hlaváč[1*], Jan Blažek[2] and Georgii Sirotenko[3]

[1] Centrum výzkumu Řež s.r.o., Brno, Czechia
[2] Institute of Information Theory and Automation of the CAS, Prague, Czechia
3 Faculty of Mathematics and Physics, Charles University, Czechia
*zbynek.hlavac@cvrez.cz

Abstract. Nuclear energy has several difficulties connected to the production or storage of the radioactive waste. Long-term operation is a process that may prolong the serviceability of the power plant by 10, 20 or more years. Nevertheless, crucial components as the reactor pressure vessel or its surrounding must be proved before enabling this process.

Fast-neutron radiation can have several effects on the concrete biological shield around a nuclear reactor. It can cause changes in the lattice structure of some rock forming minerals, resulting in an increase in volume of several percent and this may lead to cracks between the hardened cement paste and the coarse aggregate grain. Fast neutron radiation is converted in concrete to thermal neutrons which generate secondary gamma radiation and heat whereas gamma generates heat as well. Heat followed by drying causes additional shrinkage of the hardened cement paste. All these affects can be observed via digital images processing after the images have been subjected to segmentation, preprocessing, registration and normalization of the illumination.

Twelve small holes were drilled in the concrete slab 50 × 50 × 5 cm and the resulting cores of a diameter 4 cm were removed. They were cleaned and polished then inserted into the LVR-15 Research Nuclear Reactor for one year of irradiation with exposure to a flux of $6 \div 7 \times 10^{11}$ neutrons$\cdot$cm^{-2}s^{-1}.

The samples were measured and photographed using the Vertex measuring system before and after irradiation and they were examined to find evidence of any visual changes. The work on digital image processing began in April 2023 and the first outcomes should be available at the end of the year 2023.

Keywords: Crack Detection, Crack Evaluation, Digital Image Processing, Concrete Testing, Neutron Irradiation.

1 Introduction

Many sources of energy are limited these days, not only in Europe but also in many other countries all over the world. The price of all types of energy is rising and new sources are being sought. At this time many operational nuclear power plants face the problem of lifetime extension. This is called Long Term Operation (LTO) and is a problem, not only in nuclear power plants, but in all types of power plant. This paper is targeted towards LTO in nuclear power plants (NPPs) and especially towards the LTO of the shielding concrete [1]. The concrete biological shield (CBS) surrounds the active zone of the nuclear reactor, the reactor core. It must shield the surrounding area from gamma rays [2-7], damp the fast neutrons [8-10] and change them into thermal neutrons [11]. Finally, it must absorb the thermal neutrons which turn in heat [12-15] and secondary gamma radiation. This process is termed the biological protection of the nuclear reactor. Its aim is to protect the personnel in the power plant as well as those in the surrounding neighborhood.

Recent knowledge about the radiation shieling properties of the CBS is insufficient and need to be increased. The aim of this paper is to introduce the methodology of visual inspection of irradiated concrete samples, purposed as a witness specimens or coming from the accelerated studies of radiation impacts on the concrete properties. This may help to the understanding to the degradation mechanism and increase the knowledge necessary for the life-time extension of NPPs. There are not many non-destructive ways of determination the state of CBS known in the world, e.g. [16, 17], so here subjected visual inspection can help at least to investigate the irradiated samples and discover some gaps in the recent knowledge.

2 Biological shield of nuclear reactor

To ensure safe LTO the biological shield needs to be checked, as does the rest of the NPP. When the operational age of the NPP exceeds its design age, usually 40 years, the shielding concrete, which tends to be designed for the same operational life, must still be able to withstand the gamma dose, a pre-determined number of fast neutrons, the neutron fluence of a particular energetic spectra. This task determines the geometry and the composition of the concrete in the reactor pressure vessel (RPV) cavity, and the CBS wall (Fig. 1).

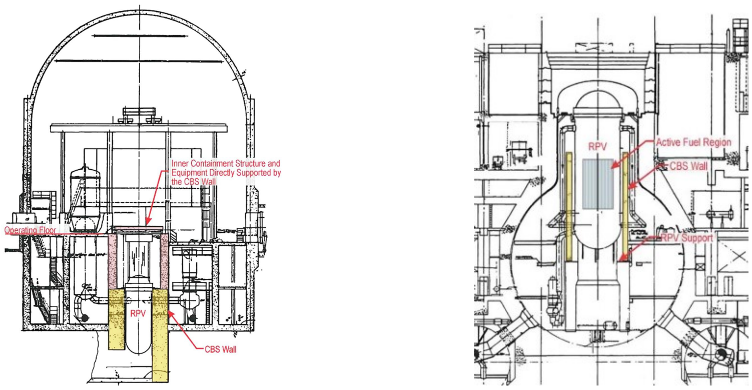

Fig. 1. Configuration of the RPV cavity and Concrete Biological Shield for a pressurized water reactor (left) and boiling water reactor (right). [1]

Concrete is a composite material that mainly consists of water, cement and additives, fine and coarse aggregates, with other admixtures or special fillers. For use as biological shielding concrete the exact types and amounts of cement, additives and especially the coarse aggregates are prescribed.
Neutron flux causes changes in the lattice of some minerals, it causes their volume increment and this initiates cracking between the hardened cement paste and the coarse aggregate grain.

3 Sample treatment and measurements

Small concrete cores 50 × 40 mm were bored out of a 500 × 500 × 50 mm concrete slab. The concrete slab was designed to prove the radiation shielding properties of a mortar, with or without cracks. The mortar was made of mixed cement CEM II 32.5, fine silicious aggregate 0 ÷ 2.5 mm and water. The testing methodology and mechanical properties of this concrete exposed to four different levels of mechanical stress were published during the 13th MBMST conference in Vilnius [18].
The 12 core samples were brushed and polished so that they fit into a special aluminum capsule which was inserted into the LVR-15 nuclear research reactor [19] and were then irradiated by fast neutrons at a fluence of 1.4×10^{19} neutrons/cm^2 (Fig. 2).

a) b)

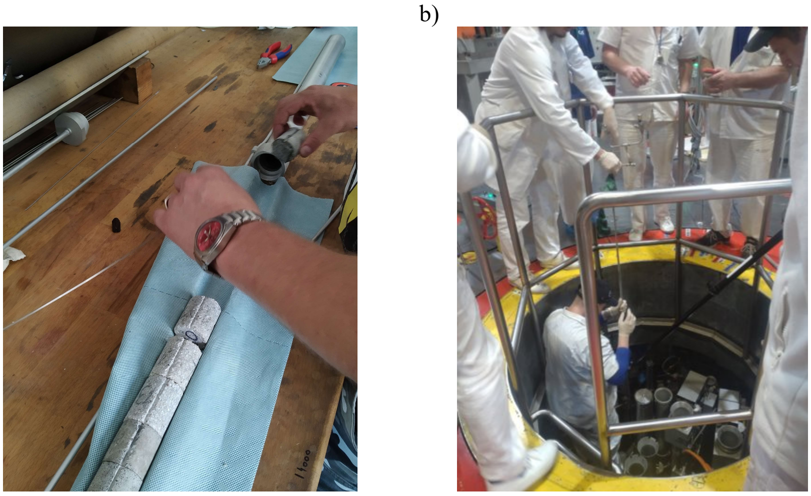

Fig. 2. The insertion of the samples into the capsules a) and then placement in the LVR-15 research reactor b).

The concrete cores were measured and photographed in the hot cells at the Research Centre Rez [20] before and after irradiation, in order to record any potential changes in the matrix due to the neutron fluence (Fig. 3). The measurement was executed by the 3D measuring Vertex system [21].

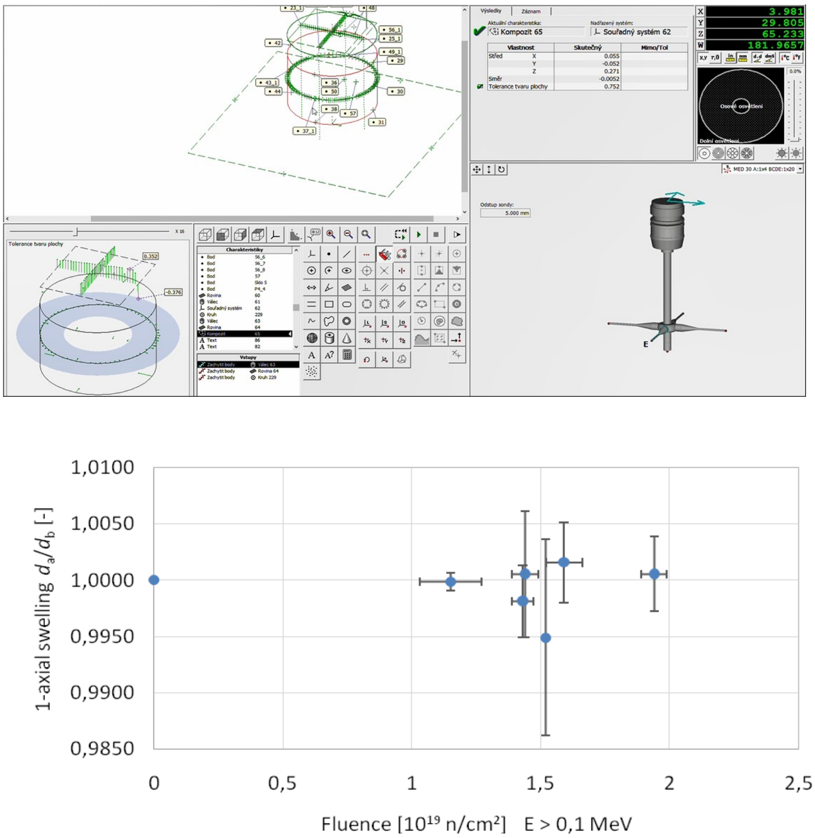

a)

b)

Fig. 3. Measurement of dimensions in the hot cell using the Vertex measuring system a); relative change of concrete cylinders' diameter d_a /d_b **a**fter and **b**efore the irradiation b).

4 Digital image processing

4.1 Data quality and simulations

Image processing algorithms are highly dependent on the quality of the input images, to address this we created phantoms (images generated by algorithms) to allow us to keep all the parameters under control. This way the hypotheses can be tested without the rejection of the results due to low image quality. In the synthetized dataset (Fig. 4), the noise, compression, visibility of cracks, etc. can be controlled.

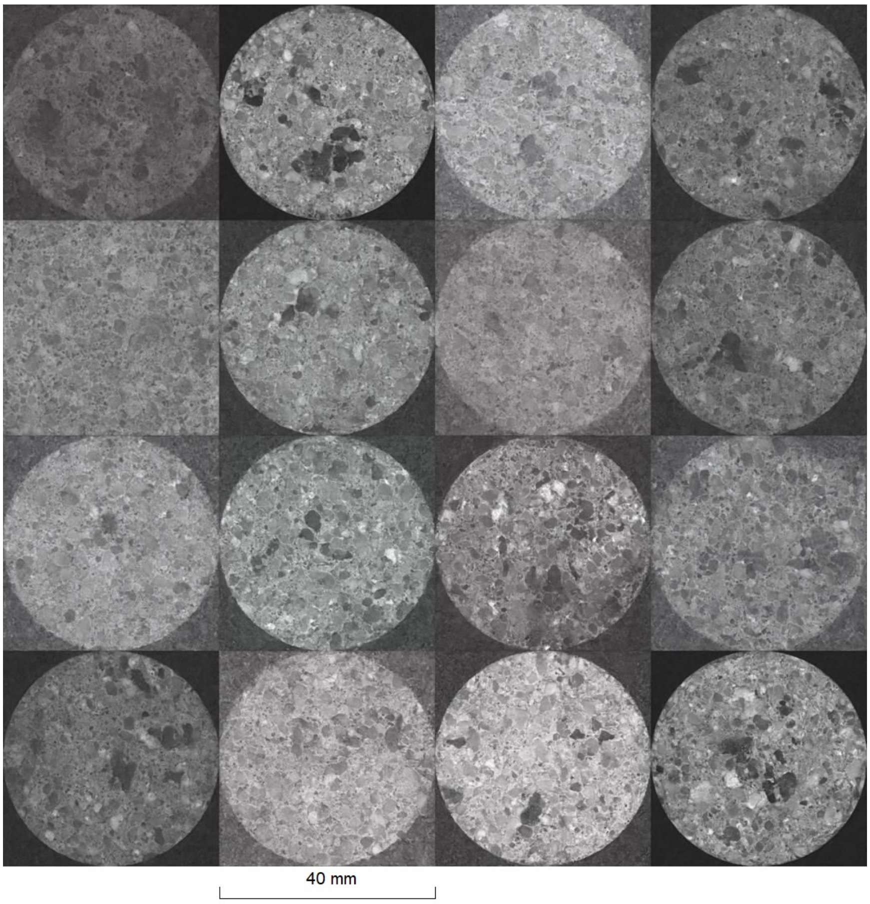

Fig. 4. A sample of the synthetized data. The quality of this dataset was controlled which made it possible to measure the quality of our input data.

4.2 Segmentation

We assume that cracks in the concrete will be visible in the macroscopic images. The data required to quantify crack growth is two macroscopic images of the same concrete sample. The first image taken prior to irradiation and the second image post irradiation. If changes are visible in the images, that means the intensity of the corresponding pixels within the two images are different due to crack growth. We assume that no other changes have occurred in the sample. The goal of automation is to develop an algorithm that will detect the changes that correspond to newly formed cracks in the pixels of the image. The second requirement is the detection of the grains, and the cement fillers between the grains, in images taken before and after irradiation and to compare their edges, size, and number. Using these strong assumptions, simple image subtraction can be used, combined with an appropriate threshold, to identify those segments that have changed between the two images. The properties of these segments are then quantified: their length and width, area, number, and color (see below). This quantifies the destruction caused by irradiation.

4.3 Pre-processing

In order for the image subtraction to be effective, it is first necessary to normalize both images. In practice this means:

1. Image registration (bringing them to the same orientation, size, and projection).
2. The normalization of the brightness of the images in all parts of the image.
3. Elimination of deviations in the images not caused by cracks (noise, lossy compression, mechanical damage to the sample).

Ideally, both images should be acquired using the same scanning device, with the same illumination, from the same position, and with lossless compression used for storage. This would eliminate points 1 and 2 above, allowing a map of the damage to be obtained through a simple image subtraction. However, in the real world, for several reasons the situation is not be so simple:

a) There may be a non-trivial time delay between the images.
b) The settings of the scanning device may not have been accurately preserved/accurately restored.
c) The position of the sample cannot be sufficiently well fixed in the scanner, resulting in differences between the positions the images are taken from.
d) A calibrated light source was not used for imaging.
e) The illumination of the sample was not uniform.
f) The image was compressed using lossy compression (JPEG artifacts).
g) The noise profile is different for each image (differences in the environmental temperature/humidity, the sensor wear/cleanliness, the temperature of the light source, etc.).

These limitations need to be compensated for within pre-processing – the normalization of the images. The choice of suitable algorithms depends on the quality of the data. Given the early stage of the project, it makes sense to focus on the normalization of the image illumination and registration. The need for further pre-processing steps will depend on the initial results.

4.4 Registration

There are a number of algorithms available for image registration. In general, there are two categories to choose from semi-automatic registration and automatic registration. At this stage, we are opting for semi-automatic registration, which requires input from the operator. This approach is more robust and will alert us to the validity or otherwise of the assumptions mentioned above.

Registration proceeds in three steps:

i. The operator selects several grains that correspond to each other in the images that have sufficient contrast.
ii. A segmentation algorithm finds the edges of the grains and calculates the position of their centroids (which should correspond in the images; minor inaccuracies due to differences in the sample before and after irradiation can be eliminated by selecting a larger number of grains).
iii. The centroid positions are unified using an appropriate global transformation (rigid, perspective, spherical).

4.5 Normalization of illumination

Uniform illumination across images is crucial for grain and crack segmentation, not only when using a naive subtraction algorithm. A lack of normalization of the images then requires the use of custom parameters to allow the segmentation of each image, and even with valid settings, discrepancies in the outputs can be expected. Therefore, this is a fundamental step in the pre-processing of images. With the data we have acquired, only relative normalization can be performed, as there are no reference images available of the sensor without illumination and a reference white surface. We assume that the scanner settings maximize the size of the sample, the sharpness of the image, and the contrast of the displayed grains, and thus the transformation of the brightness from one image to another will not reduce its clarity. With these input conditions, histogram equalization [22, pages 142-167] would be a suitable algorithm for illumination normalization, where the brightness values of one image are spread according to the histogram of the brightness values of the second image. We only consider and work on the part of the image that includes our sample (Fig. 5).

.

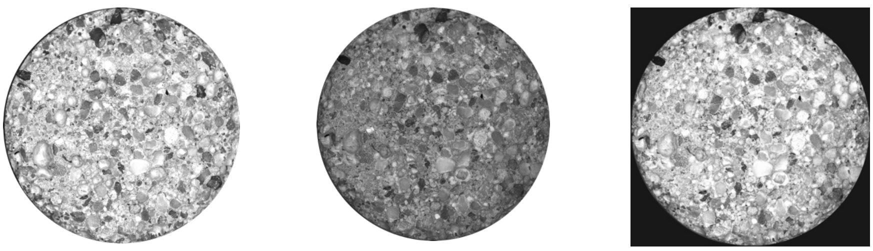

a) **b)** **c)**

Fig. 5. Normalization of illumination: reference image to which the illumination will be matched a); original image, will have its illumination normalized b); the modified version of the middle image intended to match the illumination of the reference image c).

If there is non-uniform illumination of the sample, the procedure must be applied to the images, after registration, with a local floating window [23]. The size of the window can be determined experimentally (the quickest solution) or estimated from the entire set of images that have the same pattern of illumination.

4.6 Evaluation of segmented cracks

The image of the differences has an appropriate threshold applied which allow a binary mask of the cracks to be obtained. This mask is then divided into connected regions - the cracks. For each crack, we perform skeletonization using the medial axis [24], from which we can measure the distance to the edge of the crack. Each crack is characterized using the following parameters:

1. The number of pixels that make up the crack - area
2. The distance between the mutually most distant pixels in the crack's skeleton - length
3. The maximum distance from the edge of the crack to the medial axis - maximum width
4. The average distance from the edge of the crack to the medial axis - width
5. The number of segments in the skeleton and their length - complexity of the crack. In addition, we also determine the number of cracks in the sample.

The descriptors, area, length, maximum width, width, and number of segments in the skeleton, show characteristics that continue to increase. The number of cracks in the sample increases until the cracks start to merge, after which the number decreases. The length of the skeleton segments also increases, but only until the number of branches in the skeleton and the width of the crack start to increase, after which it decreases.

Individual samples are characterized using these descriptors, and the evaluation is left to the operator.

5 Conclusions

Due to neutron irradiation, changes take place in the lattice of rock forming minerals, e.g., quartz (SiO_2) which have an atomic bond which is sensitive to neutron or gamma radiation. This leads to changes in the phase of the mineral, e.g., quartz-α → amorphous quartz, and thus to the so called RIVE (Radiation-Induced Volumetric Expansion).

RIVE in concrete is exhibited by cracking around the coarse aggregates. This is caused by the difference between the shrinkage of the hardened cement paste (HPC) and the potential swelling of rock.

The growth of the rock, HCP shrinkage, or boundary cracking can be observed via digital image processing.

This article adumbrates the methodology for the segmentation, pre-processing, registration and normalization of these images.

Project CANUT II, which is intended to unravel this particular problem, started in February 2023. It is expected to end in June 2026. “Hopefully”, cracking, RIVE or shrinkage will take place in the observed concrete samples. To date no macroscopic or visual changes have been found, but the digital image processing has just started.

Acknowledgement

This work on image processing is supported by the AV21 Strategy of the Czech Academy of Sciences as part of the research program “Breakthrough technologies of the future”.

Irradiation was performed under project VI20192022154 “Testing of biological shielding concrete after irradiation in a nuclear reactor” which received financial support from the state budget through the Ministry of the Interior of the Czech Republic as part of the Program Security research of the Czech Republic 2015-2022.

Hot sample measurement, photography and handling was provided by the project TN02000025 supported by the Technology Agency of the Czech Republic in the program National Centres of Competence 2.

References

1. Bruck P. M., Esselman T. C., Elaidi B. M., Wall J. J., Wong E. L. (2019) Structural assessment of radiation damage in light water power reactor concrete biological shield walls. *Nucl. Eng. Des*., 350, pp. 9–20.
2. Vodák, F., Trtík, K., Sopko, V., Kapičková, O., and Demo, P., (2005). ”Effect of γ-irradiation on strength of concrete for nuclear-safety structures.” *C.& Conc. Res.*, 35(7), 1447-1451.
3. Vodák, F., Vydra, V., Trtik, K. and Kapičková, O., (2011). “Effect of gamma irradiation on properties of hardened cement paste.” *Materials and Structures*, 44 (1), 101-107.
4. Łowińska-Kluge, A. and Piszora, P., (2008). “Effect of gamma irradiation on cement composite observed withXRD and SEM methods in the range of radiation dose 0-1409 MGy.” *ActaPhysicaPolonica*, 114(2), 399-411.
5. Kontani, O., Sawada, S., Maruyama, I., Takizawa, M. and Sato, O., (2013). “Evaluation of irradiation effects on concrete structure—Gamma-ray irradiation tests on cement paste.” *Proceedings of the ASME 2013 power conference: Power2013*, Boston, New York: Am. Soc. of Mech.Engrs, 29 July-1 August 2013: Paper no. 98099, V002T07A002.
6. Koťátková, J., Hlaváč, Z., Rosnecký, V., Mohyla, R. and Jansa, J., (2018). “The effect of superplasticizers on the properties of gamma irradiated cement pastes.”*Ceramics - Silikáty*, 62 (3), 306-310.
7. Koťátková, J.,Zatloukal, J., Reiterman, P.,Kolář, K. and Hlaváč, Z., (2018).“H2 Generation in Cement Pastes under Gamma Irradiation – A State of the Art.”*Materials Structures Technology*, 1 (1), 18-25.
8. Maruyama, I., Kontani, O., Sawada, S., Sato, O., Igarashi, G. and Takizawa, M., (2013). “Evaluation of irradiation effects on concrete structure—background and preparation of

neutron irradiation test." *Proceedings of the ASME 2013 power conference POWER2013*, Boston, USA, 29 July-1 August 2013: number 98114.

9. Le Pape, Y. , (2015). "Structural effects of radiation-induced volumetric expansion on unreinforced concrete biological shields." *Nuclear Engineering and Design*,295, 534-548.
10. Hlaváč, Z., Zatloukalová, J., Brabec, P., Černoušek, T. (2022) Investigation of nuclear concrete, In *NDT.net Journal, e-Journal of Nondestructive Testing (NDT),* pp. 1–9. https://www.ndt.net/search/docs.php3?id=27282, last accessed 2023/05/04.
11. Košťál, M., Milčák, J., Rypar, V., Juříček, V., Novák, E., Kolros, A., Cvachovec, F. and Zaritski, S., (2014). "The Effect of Concrete Shielding on Neutron Transport in the VVER-1000 Mock-Up," *Progress in Nuclear Science and Technology*, 4, 317–321.
12. Maruyama, I., Kontani, O., Ishizawa, A., Takizawa, M. and Sato, O., (2012). "Development of system for evaluating concrete strength deterioration due to radiation and resultant heat." *Proceedings of 3rd international conference on NPP life management for long term operations*, Salt Lake City,USA, May 2012: IAEA-CN-194-096.
13. Maruyama, I., Nishioka, Y., Igarashi, G., and Matsui, K., (2014). "Microstructural and bulk property changes in hardened cement paste during the first drying process." *Cement and Concrete Research*, 58(0), 20-34.
14. Maruyama, I., Sasano, H., Nishioka, Y. and Igarashi, G., (2014). "Strength and Young's modulus change in concrete due to long-term drying and heating up to 90°C." *Cement and Concrete Research*, 66(0), 48-63.
15. Koťátková, J., Zatloukal, J., Reiterman, P., Patera, J., Hlaváč, Z. and Brabec, P., (2016)"The Effect of Elevated Temperatures and Nuclear Radiation on the Properties of Biological Shielding Concrete."*Key Engineering Materials,* 677 (Jan), 8-17.
16. Patera, J., Žďárek, J., Zárybnická, E. et al. (2023) Non-destructive testing of mock-up of reactor pressure vessel cavity, In *Proceedings of the International Conference on Non-destructive Evaluation of Concrete in Nuclear Applications,* pp. 148–154. https://www.ndt.net/search/docs.php3?id=27817, last accessed 2023/05/04.
17. Hlaváč, Z., Khmurovská, Y., Halodová, P. et al. (2023) Non-destructive testing of coarse aggregates irradiated by neutron and gamma radiation for the European project ACES, In *NDT.net Journal, e-Journal of Nondestructive Testing (NDT),* pp. 315–326. https://www.ndt.net/search/docs.php3?id=27836, last accessed 2023/05/11.
18. Koťátková, J., Patera, J., Hlaváč, Z. (2019) Non-linear Ultrasonic Defectoscopy of Concrete Structures for Nuclear Industry, In *Selected papers of the 13th International Conference Modern Building Materials, Structures and Techniques*, pp. 373–378, Vilnius.
19. LVR-15 reactor's homepage, http://reaktory.cvrez.cz/en/research-reactor-lvr-15, last accessed 2023/05/03.
20. The hot cells' home page, https://www.cvrez.cz/cs/vyzkum-a-sluzby/provoz-reaktoru/horke-komory-12202, last accessed 2023/05/04.
21. The Vertex home page, https://www.microvu.com/machines/vertex, last accessed 2023/05/04.
22. Gonzalez R. C., Woods R. E. (2008) Digital Image Processing, Third Edition, pp. 142–161.
23. Pizer S. M., Amburn E. P., Austin J.D. et al. (1987) Adaptive Histogram Equalization and Its Variations, *Comp. Vis., Graphics, & Im. Proc.* 39, pp. 355–368.
24. The medial axis morphology home page, https://scikit-image.org/docs/stable/api/skimage.morphology.html#skimage.morphology.medial_axis, last accessed 2023/04/17.